Solid State Science and Technology, Vol. 30, No 1 & 2 (2022), 20-36
ISSN 0128-7389 | *http://myjms.mohe.gov.my/index.php/masshp*

FIRST-PRINCIPLE LDA+U AND GGA+U CALCULATIONS ON STRUCTURAL AND ELECTRONIC PROPERTIES OF WURTZITE ZnO

N. Hamzah[1], M. H. Samat[2], N. A. Johari[1], A. F. A. Faizal[1], O. H. Hassan[2,3], A. M. M. Ali[2,4], R. Zakaria[2,4], N. H. Hussin[5], M. Z. A. Yahya[6] and M. F. M. Taib[2,4]

[1]*Centre of Foundation Studies, Universiti Teknologi MARA, 43800 Dengkil, Selangor, Malaysia*

[2]*Ionic Materials & Devices (iMADE) Research Laboratory, Institute of Science, Universiti Teknologi MARA, 40450 Shah Alam, Selangor, Malaysia*

[3]*Department of Industrial Ceramics, Faculty of Art & Design, Universiti Teknologi MARA, 40450 Shah Alam, Selangor, Malaysia*

[4]*Faculty of Applied Sciences, Universiti Teknologi MARA, 40450 Shah Alam, Selangor, Malaysia*

[5]*Faculty of Applied Sciences, Universiti Teknologi MARA, 26400 Jengka, Pahang, Malaysia*

[6]*Faculty of Defence Sciences and Technology, Universiti Pertahanan Nasional Malaysia, 57000 Kuala Lumpur, Malaysia*

**Corresponding authors*: *mfariz@uitm.edu.my*

Received: 4 January 2022; Revised: 8 August 2022; Accepted: 12 September 2022

ABSTRACT

First-principles calculations with density functional theory (DFT) were carried out to explore the effects of Hubbard on-site Coulombic correction on the structural and electronic properties of wurtzite zinc oxide (ZnO). For an accurate prediction of ZnO properties, adequate Hubbard terms must be established due to changes in structural parameters produced by the correction of hybridization between Zn 3*d* and O 2*p* states. The calculations are based on the local density approximation (LDA) and the generalized gradient approximation (GGA) for Perdew-Burke-Ernzerhof (PBE) and Perdew-Burke-Ernzerhof for solids (PBEsol) were performed by applying Hubbard corrections U_d to Zn 3*d* states and U_p to O 2*p* states. The lattice parameters were closer to the experimental data and underestimated when Hubbard corrections U_d and U_p were applied in the calculation. The combination of the correction terms U_d and U_p managed to improve the underestimated bandgap of wurtzite ZnO, which might solve the

standard DFT problems. The best Hubbard parameters U_d and U_p found for LDA+U at U_d = 6 eV and U_p = 8 eV, GGA-PBE at U_d =2 eV and U_p = 10 eV and GGA-PBEsol+U at U_d = 5 eV and U_p = 9 eV show a good agreement with the experimental bandgap.

Keywords: Wurtzite ZnO, first-principles, density functional theory, Hubbard correction, electronic

INTRODUCTION

Zinc oxide (ZnO) is a compound semiconductor belonging to the II-VI groups with a direct bandgap of 3.37 eV and a higher exciton binding energy of 60 meV at room temperature [1,2]. ZnO has attracted much attention due to its potential application in solar cells, photocatalyst, optoelectronic devices, semiconductor laser and light-emitting diodes [3–7]. ZnO has a stable wurtzite crystal structure under ambient conditions. Nevertheless, at relatively high pressure, the ZnO has observed a rock-salt crystal structure and ZnO is stabilized by the growth of a zinc-blende crystal structure on a cubic substrate [8].

The computational method based on density functional theory (DFT) has successfully treated the structural, electronic, and optical properties of ZnO [9–11]. The DFT calculations focused on local density approximation (LDA) and generalized gradient approximation (GGA) are practical methods to simulate relatively large structures with sufficient chemical precision. However, the standard DFT approach focused on the exchange-correlation (XC) functionals of the LDA and GGA yields underestimated value bandgap energy for some semiconductors [12,13]. DFT calculations report a bandgap of ZnO is (0.65 – 0.74 eV), which is underestimated by ~70% compared with the experimental value is (3.37 eV) [14–17]. The apparent error in the calculation of energy bandgap failed to describe the localization of strongly correlated electronic *d* and *f* electrons metals [18,19].

The hybrid functionals or DFT+U methods are the most commonly utilized approaches to overcome the problems of standard DFT [20]. The Green's function and screened Coulomb's potential (GW) and hybrid functionals like Perdew-Burke-Ernzerhof (PBE0), Heyd-Scuseria-Ernzerhof (HSE06) and Becke, 3-parameters, Lee-Yang-Parr (B3LYP) are a popular approach to be more accurate in the calculation of the energy bandgap of ZnO [9,21,22]. However, hybrid functionals are considered to require higher computing costs [23]. Therefore, the first-principle method based on DFT+U is a barely suitable approach due to the less expensive computational method and low difficulty level. Nevertheless, applying the Hubbard U_d correction only to the *d* state, the bandgap of ZnO is still underestimated, even at large U_d values [24,25]. Numerous recent theoretical studies have investigated the influence of the Hubbard parameter U_d on the *d* state of Zn and U_p on the *p* state of oxygen (O) can improve the bandgap and position of the valence and conduction band when both Hubbard parameters U_d and U_p are used [26–29]. Therefore, the Hubbard parameters U_d and U_p values need to be rationally correct in order to obtain more accurate structural parameters and electronic properties of ZnO.

In this work, the aim is to determine the suitable values of Hubbard parameters U_d and U_p using first-principles calculation within the DFT+U (LDA+U, GGA-PBE+U and GGA-PBEsol+U) framework, which depends on structural (lattice parameters and volume) and electronic (band structures and total and partial density of state) properties of wurtzite ZnO. Different values of the Hubbard parameters U_d and U_p are used to do a series of DFT+U calculations. The results from inclusion Hubbard parameters U_d and U_p on DFT+U calculations were compared with those calculated using standard DFT and experimental data. A similar work of inclusion Hubbard parameters U_d and U_p on DFT+U calculation of wurtzite ZnO had been carried out, but only using LDA+U functional and different computational software [28].

COMPUTATIONAL DETAIL

First-principles calculations based on plane-wave ultrasoft pseudopotentials method were performed for wurtzite ZnO using Cambridge Serial Total Energy Package (CASTEP) module in Materials Studio (MS) 8.0 developed by Accelrys Sofware Inc [30,31]. The structural and electronic properties of wurtzite ZnO were calculated using XC functionals from LDA by Ceperley and Adler as parametrized by Perdew and Zunger (LDA-CAPZ) and GGA of Perdew-Burke-Ernzerhof (GGA-PBE) and Perdew-Burke-Ernzerhof for solids (GGA-PBEsol) [13,32,33]. The valence electron configurations were treated as Zn-4$s^2$3d^{10} and O-2$s^2$2p^4. The optimized cut-off energy value for the plane-wave basis set of the electronic wave function was 340 eV. The integration in the Brillouin zone was performed using 5 × 5 × 4 *k*-points from the Monkhorst-Pack scheme. The geometrical optimization was performed using the total energy of 1.0×10^{-5} eV/atom, the maximum force of 0.03 eV/Å, the maximum stress of 0.05 GPa and maximum atomic displacement of 1.0×10^{-3} Å.

Three strategies were performed by utilizing distinct XC functionals to investigate the conceptual differences in calculation. The optimization was first performed on the unit cell of wurtzite ZnO using a standard DFT (LDA, GGA-PBE and GGA-PBEsol). In the second optimization, the Hubbard term U_d is applied to the 3*d* states of the Zn atoms using DFT+U (LDA+U, GGA-PBE+U and GGA-PBEsol+U), which the U_d values range from 1 eV to 10 eV. The third optimization process implemented both Hubbard term U_d to Zn 3*d* states and U_p to O 2*p* states using DFT+U (LDA+U, GGA-PBE+U and GGA-PBEsol+U), where the U_d and U_p values range from 1 eV to 10 eV. To provide an accurate description of the calculated structural and electronic properties of wurtzite ZnO, the DFT + U_d + U_p method were adopted according to the following formalism [26, 34];

$$E_{\mathrm{DFT+U}} = E_{\mathrm{DFT}} + \frac{\mathrm{U}-\mathrm{J}}{2}\sum_{\sigma} T_r[\rho^{\sigma}\rho^{\sigma} - \rho^{\sigma}] \qquad (1)$$

where ρ^{σ} denotes the spin (σ) polarized on-site density matrix. The spherically averaged Hubbard parameter U represents the increase of energy generated by placing an

additional electron at a certain position and the screened exchange energy is represented by parameter J (1 eV). The various values in the optimized lattice parameter and corresponding bandgap energy, E_g were investigated. The best XC functional for the ZnO system was determined through analysis.

RESULTS AND DISCUSSION

Structural Parameters

The crystal structure of wurtzite ZnO (hexagonal, space group $P6_3mc$) is visualized in Figure 1. The unit cell of wurtzite ZnO contains 4 atoms which consist of 2 zinc (Zn) and 2 oxygen (O). The crystal structures of wurtzite ZnO were optimized by minimizing the total energy and atomic forces. Optimization was carried out utilizing several approximations in order to identify the best functional for the ZnO system. The lattice parameters (*a* and *c*), lattice ratio (*c*/*a*) and volume (V) of optimized wurtzite ZnO computed from standard LDA, GGA-PBE and GGA-PBEsol functionals were compared to the experimental values were listed in Table 1. The value of lattice parameters from standard LDA was found underestimates (1.37% – 1.82%) the values of lattice parameters from the standard of GGA (0.10% – 1.91%). In contrast, the value of lattice parameters GGA-PBE and GGA-PBEsol were consistent with each other, which agrees with other findings [35–37]. The lattice parameters and volume from GGA-PBEsol show a good agreement with the experimental values, which is less than 0.59% deviation compared to the other calculated lattice parameters and volume from standard LDA and GGA-PBE functionals.

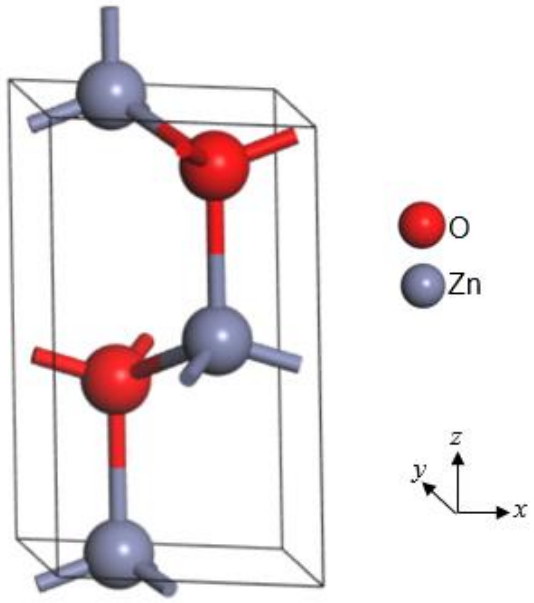

Figure 1: Crystal structure of unit cell for wurtzite ZnO

Table 1: The calculated lattice parameters (*a* and *c*), lattice ratio (*c*/*a*) and volume (V) of wurtzite ZnO using standard LDA, GGA-PBE and GGA-PBEsol with the percentage deviation from the experiment and other theoretical data

	Method						
	Present works			Other works [35–37]			Experiment [38,39]
	LDA	GGA-PBE	GGA-PBEsol	LDA	GGA-PBE	GGA-PBEsol	
a (Å)	3.1907 (–1.82%)	3.2888 (+1.20%)	3.2466 (–0.10%)	3.1860	3.2819	3.2710	3.2499
c (Å)	5.1598 (–1.37%)	5.3056 (+1.91%)	5.2317 (+0.49%)	5.1500	5.2943	5.2350	5.2063
c/*a*	1.6172 (+0.95%)	1.6132 (+0.70%)	1.6115 (+0.59%)	1.6200	1.6130	1.6000	1.6020
V ($Å^3$)	45.492 (–4.42%)	49.699 (+4.42%)	47.755 (+0.33%)	45.270	49.386	47.759	47.597

(+) overestimate; (–) underestimate

The effects of inclusion Hubbard parameter U_d applied to the 3*d* states of the Zn on the lattice parameters and volume of wurtzite ZnO was investigated by optimizing the crystal structures using LDA+U, GGA-PBE+U and GGA-PBEsol+U functionals. The lattice parameters *a* and *c* and volume gradually increased with the increment in the Hubbard parameter U_d range from 1 eV to 10 eV from LDA+U, GGA-PBE+U and GGA-PBEsol+U functionals as in Figure 2, in agreement with the result produced in similar research using CASTEP software by other theoretical researchers [24,35,37]. Figure 2 (a) shows that at U_d = 2 eV, lattice parameter *a* from the GGA-PBEsol+U functional value is equal to the experimental value 3.2499 Å, which represents by horizontal dash lines [38]. However, the trend lines of lattice parameters *c* and volume in Figure 2 (b) and (c) never reach the point of the experimental values, which are 5.2063 Å and 47.597 $Å^3$ [39]. Therefore, the lattice parameters of wurtzite ZnO using the inclusion Hubbard parameter U_d applied to the 3*d* states of the Zn were best described from GGA-PBEsol+U at U_d = 2 eV for only calculation lattice parameter *a* and none for calculation lattice parameter *c* and volume. Compared with the previous standard DFT calculations, the percentage deviation of lattice parameters *a* and *c* and volume of wurtzite ZnO without the inclusion Hubbard parameter U_d is still good and below +0.49% using standard GGA-PBEsol.

The effects of inclusion Hubbard parameter U_d applied to the 3*d* states of the Zn and U_p applied to the 2*p* states of the O on the lattice parameters and volume of wurtzite ZnO was investigated by optimizing the crystal structures using LDA+U, GGA-PBE+U and GGA-PBEsol+U functionals. The lattice parameters *a* and *c* and volume gradually decreased with the increment in the Hubbard parameter U_p at all fixed values of U_d range from 1 eV to 10 eV from LDA+U, GGA-PBE+U and GGA-PBEsol+U functionals as in Figure 3, Figure 4 and Figure 5 due to stronger localization of the electron state. Using LDA+U, GGA-PBE+U and GGA-PBEsol+U functionals, similar trends are agreed by the other theoretical researchers using the same CASTEP software [40]. Figures 3 (a), 4 (a) and 5 (a) show that none of the U_d and U_p matches the experimental lattice parameters *a* and *c* and volume values. The lattice parameters *a* and

c and the volume calculated using the LDA+U functional are underestimated and further away from experimental values as the Hubbard parameter U_p increases. A similar trend is agreed by the other theoretical researchers using the same LDA+U functional but different software [28]. Meanwhile, Figures 4 and Figure 5 show that the reduction of lattice parameters *a* and *c* and the volume from GGA-PBE+U and GGA-PBEsol+U improves the overestimation from standard GGA-PBE and GGA-PBEsol.

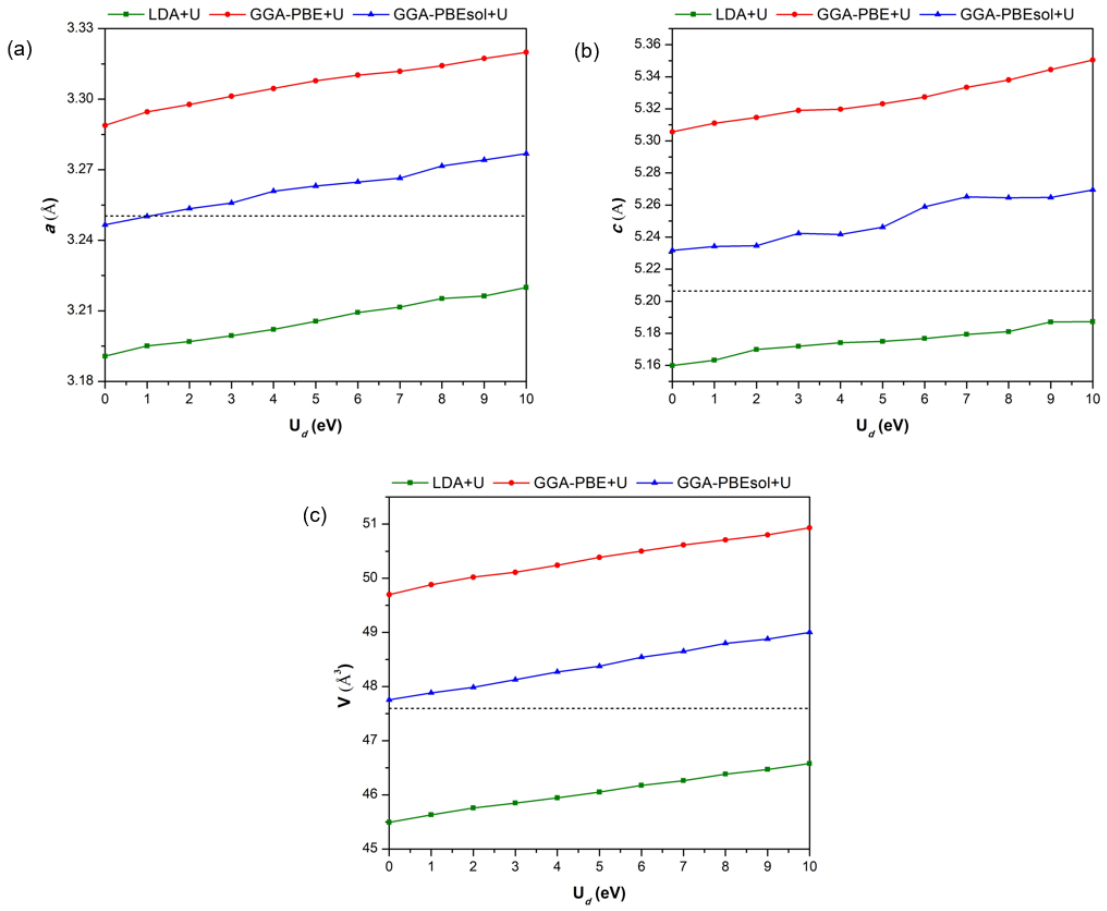

Figure 2: (a) Lattice parameter *a*, (b) lattice parameter *c* and (c) volume (V) of wurtzite ZnO with respect to Hubbard parameter U_d applied to Zn for different functionals LDA+U, GGA-PBE+U and GGA-PBEsol+U. Horizontal dashed lines represent the experimental values

From Figures 3 (b), 4 (b) and 5 (b), it show the matches lattice parameter *a* value with experimental at point U_d = 6 eV and U_p = 10 eV (0.00%), lattice parameter *c* at point U_d = 1 eV and U_p = 9 eV (+0.02%) and volume at point U_d = 6 eV and U_p = 10 eV (+0.14%), whereas Figure 3 (c), 4 (c) and 5 (c) show the matches lattice parameter *a* value with experimental at point U_d = 8 eV and U_p = 3 eV (0.00%), lattice parameter *c* at point U_d = 9 eV and U_p = 5 eV (+0.01%) and volume at point U_d = 9 eV and U_p = 4 eV (−0.07%).

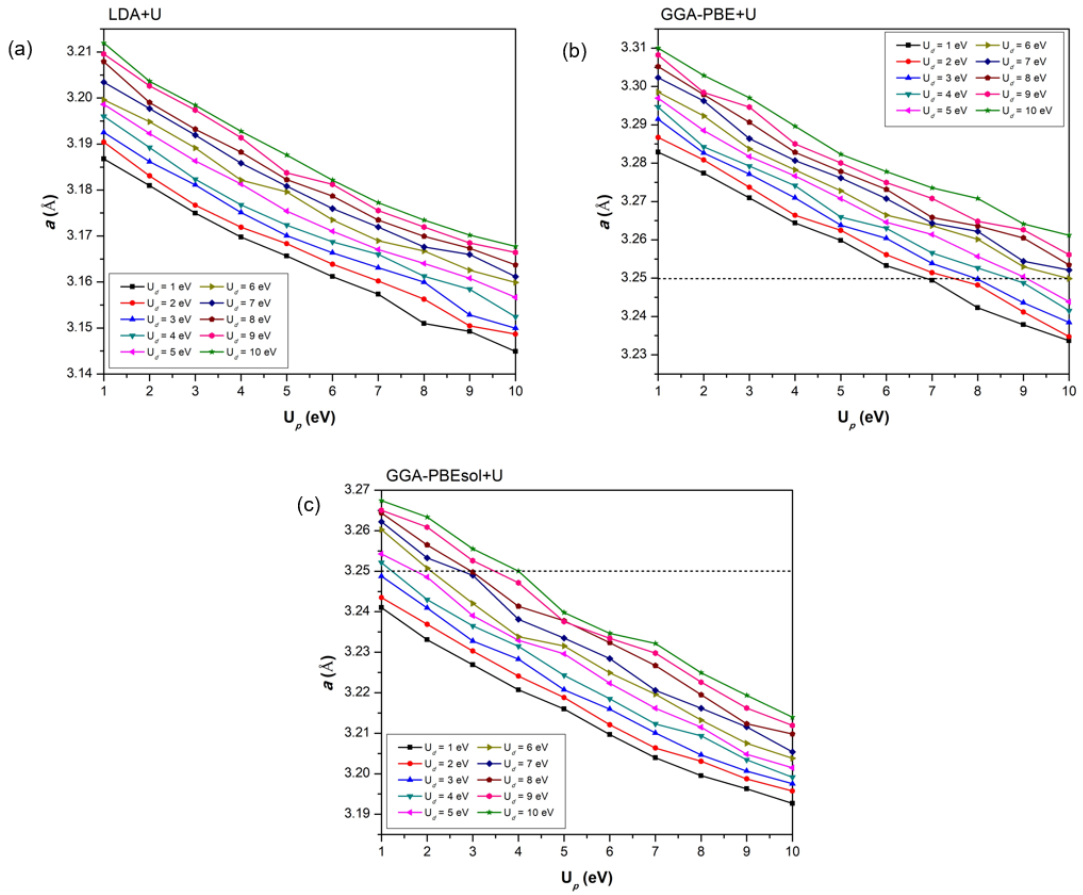

Figure 3: Lattice parameters *a* of wurtzite ZnO with respect to Hubbard parameter U_p applied to O with fixed U_d values for different functionals (a) LDA+U, (b) GGA-PBE+U and (c) GGA-PBEsol+U. Horizontal dashed lines represent the experimental Values.

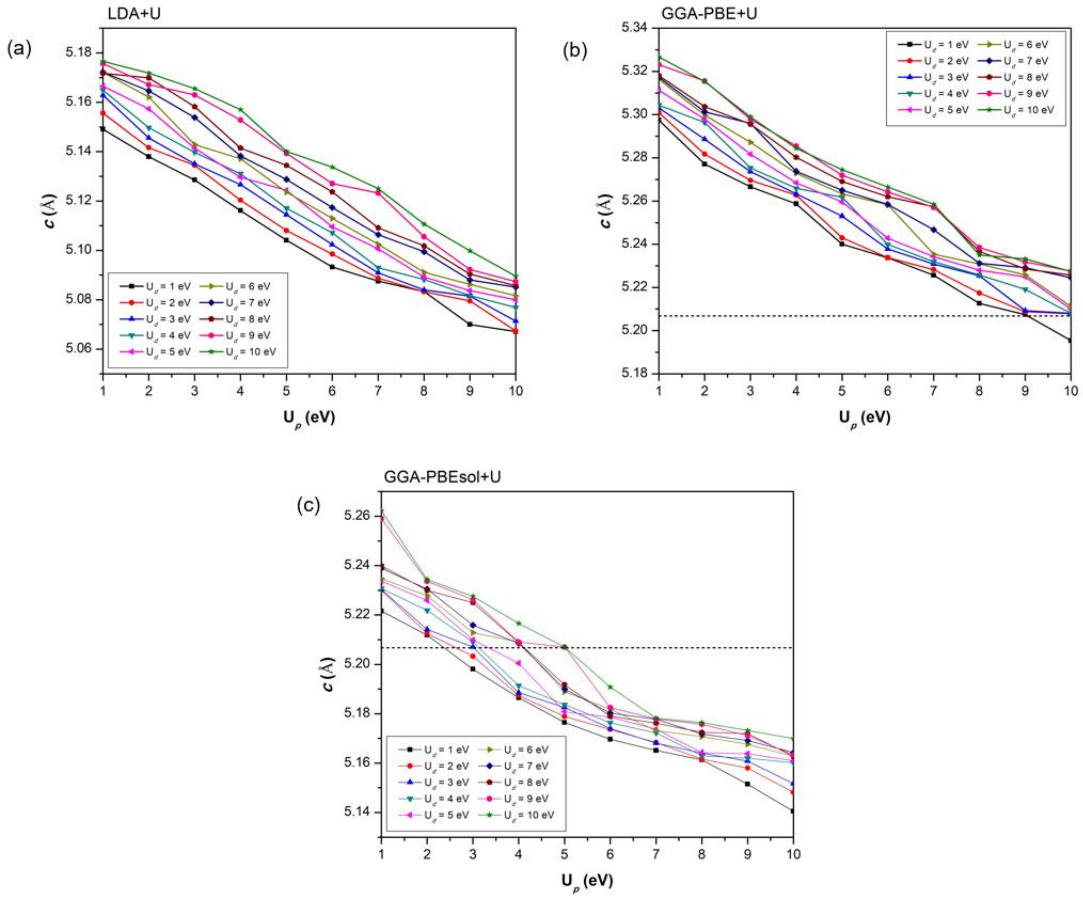

Figure 4: Lattice parameters *c* of wurtzite ZnO with respect to Hubbard parameter U_p applied to O with fixed U_d values for different functionals (a) LDA+U, (b) GGA-PBE+U and (c) GGA-PBEsol+U. Horizontal dashed lines represent the experimental values.

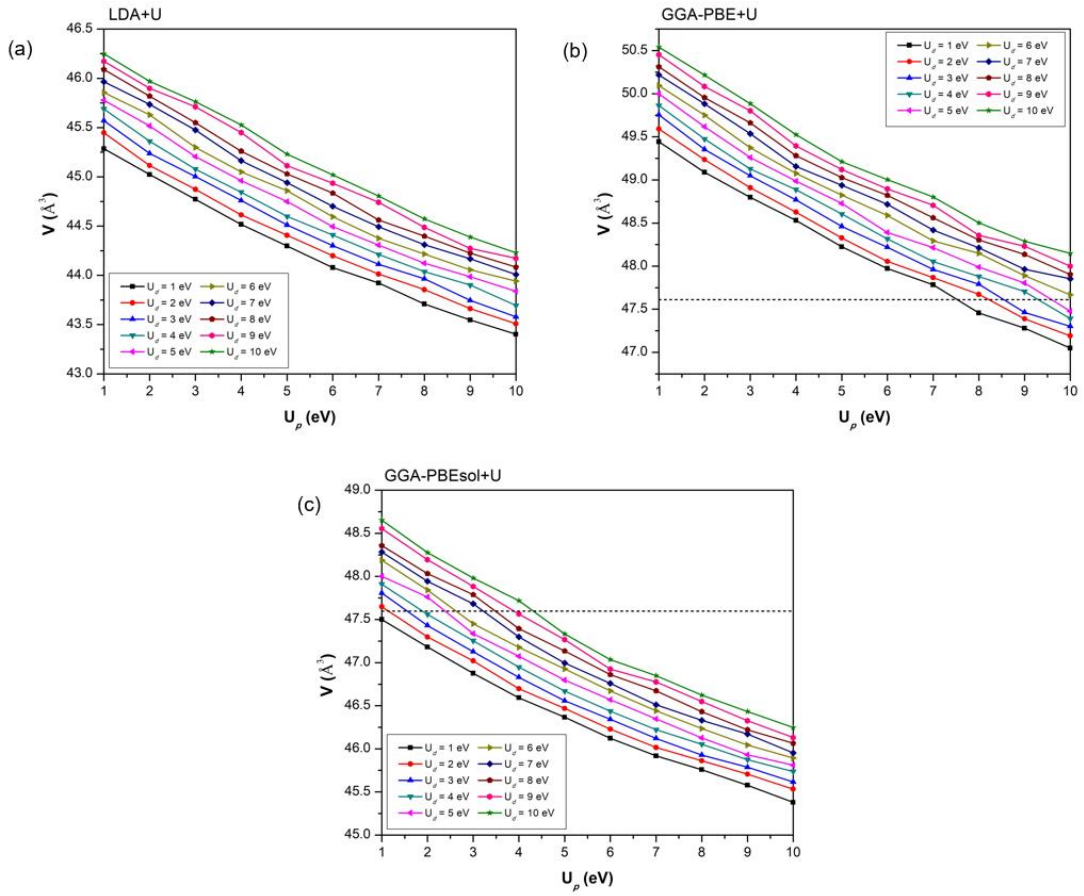

Figure 5: Volume (V) of wurtzite ZnO with respect to Hubbard parameter U_p applied to O with fixed U_d values for different functionals (a) LDA+U, (b) GGA-PBE+U and (c) GGA-PBEsol+U. Horizontal dashed lines represent the experimental values

The reduction of lattice parameter *a* with increased the Hubbard parameter U_p agreed with other theoretical researchers using the same GGA+U functional but different software [41]. It is concluded that the structural parameters of wurtzite ZnO were most aptly described from GGA-PBEsol+U with possible agreements of different Hubbard U_d and U_p values. The effects of inclusion Hubbard parameter U_d applied to the 3*d* states of the Zn and U_p applied to the 2*p* states of the O were underestimated the structural properties of wurtzite ZnO.

Electronic Properties

The calculated bandgaps energy of wurtzite ZnO using standard LDA, GGA-PBE and GGA-PBEsol functionals were found underestimated (76% – 82%) compared to the experimental values are listed in Table 2, which is agreed well with the previous DFT researches [40,42,43]. These problems are driven by standard LDA, GGA-PBE and GGA-PBEsol, that failure to locate the binding energy in the 3*d* states electrons, resulting in the overestimation of hybridization with the anion 2*p* states. Thus, a strong *p-d* coupling was finally causing the reduction of the bandgaps [41].

Table 2: The bandgap (E_g) of wurtzite ZnO using standard LDA, GGA-PBE and GGA-PBEsol and LDA+U, GGA-PBE+U and GGA-PBEsol+U with the percentage deviation from the experiment and other theoretical data

	Method	U_d/eV	U_p/eV	E_g/eV
Presents works	LDA	-	-	0.791 (–76.53%)
	GGA-PBE	-	-	0.733 (–78.25%)
	GGA-PBEsol	-	-	0.618 (–81.66%)
	LDA+U	6	8	3.364 (–0.18%)
	GGA-PBE+U	2	10	3.379 (+0.27%)
	GGA-PBEsol+U	5	9	3.365 (–0.15%)
Other works [26,40,42–45]	LDA	-	-	0.770
	GGA-PBE	-	-	0.741
	GGA-PBEsol	-	-	0.622
	LDA+U	8	7	3.310
	GGA-PBE+U	10	7	3.300
	GGA-PBEsol+U	10	7	3.370
Experiment [38,39]		-	-	3.37

(+) overestimate; (–) underestimate

The variation bandgap values of wurtzite ZnO with the inclusion of Hubbard parameter U_d applied to Zn for different functionals are presented in Figure 6. As U_d values increased from 1 eV to 10 eV, the bandgap values also increased. The highest values of bandgaps at U_d = 10 eV are 1.30 eV (LDA+U), 1.17 eV (GGA-PBE+U) and 1.11 eV

(GGA-PBEsol +U). These bandgap values are still small compared to the experimental value (3.37 eV), which agrees with previous researches even though the inclusion of the Hubbard U_d parameter aims to correct the localized 3*d* states electrons in a correlated system but is still underestimated [28,37,46]. When only the Hubbard parameter U_d was changed, a significant fluctuation in total energy was observed, indicating an incomplete representation of the bandgap structure [41].

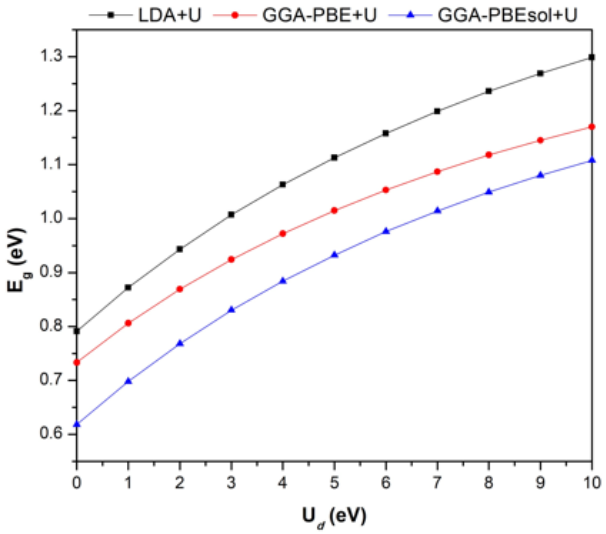

Figure 6: Dependence bandgap values of wurtzite ZnO with respect to Hubbard parameter U_d applied to Zn for different functionals LDA+U, GGA-PBE+U and GGA-PBEsol+U

The widespread underestimate in bandgap has brought to light the necessity of including the 2*p* states in the calculations. The selection of the appropriate value of U_d and U_p are required to investigate the bandgaps properties of wurtzite ZnO. Figure 7 presented the variation bandgap values of wurtzite ZnO with the Hubbard parameter U_p applied to O with fixed U_d values for different functionals. The bandgap values gradually increased with the increment in the Hubbard parameter U_p range from 1 eV to 10 eV with fixed U_d values. The matches bandgaps value with experimental is listed in Table 2. Thus, the bandgap from GGA-PBEsol+U functional nearly matched the experimental by 0.15% deviation. From the previous research, the selection of Hubbard U_d is typically in the range of 8 eV to 10 eV, whereas for U_p in the range of 7 eV, using the same CASTEP software [26,44,45]. Thus, this will prove that the inclusion of both Hubbard parameters, U_d dan U_p has successfully reproduced the correct bandgap of wurtzite ZnO compared to the standard LDA, GGA+PBE and GGA+PBEsol. The Hubbard parameters U_d and U_p values for electronic properties are not the same as the structural properties, but the problem is to correct the underestimated bandgap of wurtzite ZnO from standard DFT by inclusion Hubbard parameter U_d applied to the Zn-3*d* state and U_p applied to the O-2*p* state. The structural properties using standard DFT are still acceptable due to percentage deviation below +5.00%.

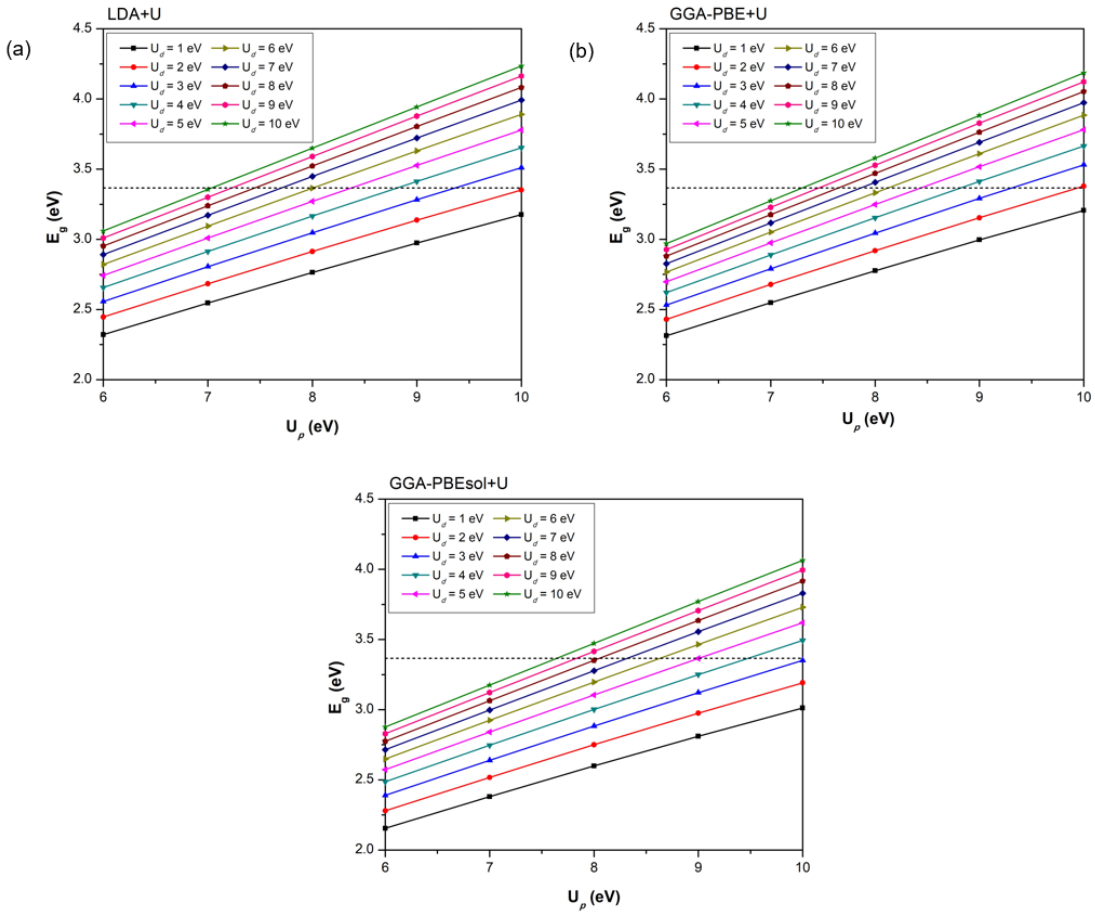

Figure 7: Dependence bandgap values of wurtzite ZnO with respect to Hubbard parameter U_p applied to O with fixed U_d values for different functionals (a) LDA+U, (b) GGA-PBE+U and (c) GGA-PBEsol+U. Horizontal dashed lines represent the experimental values

The calculated band structures of wurtzite ZnO using standard LDA, GGA-PBE and GGA-PBEsol functionals and the best Hubbard parameters U_d and U_p for LDA+U, GGA-PBE+U and GGA-PBEsol+U along the highest symmetry direction of the Brillouin zone path from G-A-H-K-G-M-L-H are presented in Figure 8. The results imply that the wurtzite ZnO has a direct energy bandgap between the G Brillouin zone valence and the conduction band. The bandgap energy is determined between the valence band maximum and the conduction band minimum, in which the Fermi level is situated at 0 eV of the energy scale. The calculated bandgaps of wurtzite ZnO from standard LDA, GGA+PBE and GGA-PBEsol were about 0.791 eV, 0.733 eV and 0.618 eV, in good agreement with the other first-principle DFT calculations [40,47,48]. Nevertheless, the bandgap results did not affect the accuracy of comparing the related crystal properties, such as band structure and density of state.

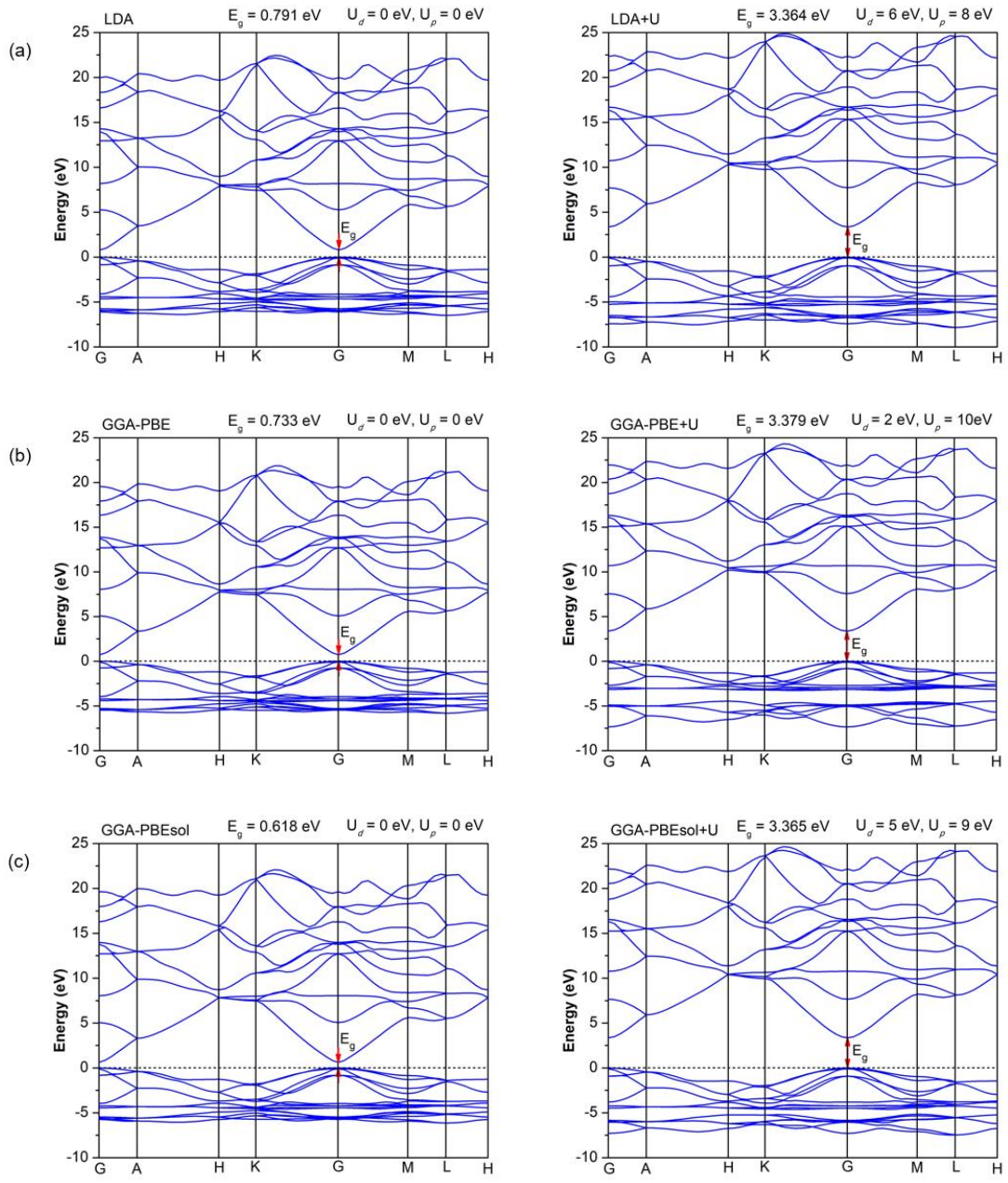

Figure 8: Comparison bandgap structures of wurtzite ZnO using different functionals (a) LDA and LDA+U, (b) GGA-PBE and GGA-PBE+U and (c) GGA-PBEsol and GGA-PBEsol+U for without Hubbard U and with the best Hubbard parameters U_d and U_p

It is well known that the underestimated bandgap can be due to the ground state DFT results of strong Columb correlation and XC potential between excited-state electrons. Underestimation of the bandgap from the first-principle calculations can be fixed using Hubbard parameter U_d and U_p to compare it with the experimental results. Therefore, the effective Hubbard parameters U_d and U_p in LDA+U, GGA-PBE+U and GGA-PBEsol+U calculations tend to upper shifted the minimum conduction band to give the

larger gap between the maximum valence band and minimum conduction band. The calculated bandgaps of wurtzite ZnO from LDA+U, GGA+PBE+U and GGA-PBEsol+U were about 3.364 eV, 3.379 eV and 3.365 eV. All the bandgaps values are in good agreement with the other first-principle DFT+U calculations [26,49,50]. Hence, the bandgap from GGA-PBEsol functional nearly matched the experimental by 0.15% deviation.

The contribution of the partial density of state (PDOS) and total density of state (TDOS) of wurtzite ZnO obtained from standard LDA, GGA-PBE and GGA-PBEsol functionals and the best Hubbard parameters U_d and U_p for LDA+U, GGA-PBE+U and GGA-PBEsol+U are illustrated in Figure 9. The PDOS and TDOS were used to analyze the contribution of the electrons from *s*, *p* and *d* orbitals in wurtzite ZnO. The calculated DOS of wurtzite ZnO for LDA, GGA-PBE, GGA-PBEsol, LDA+U, GGA-PBE+U and GGA-PBEsol+U were within energy interval from –20 eV to 25 eV and the Fermi level situated at 0 eV of the energy scale.

From the standard LDA, GGA-PBE and GGA-PBEsol, the first peak at around –17.38 eV to −17.21 eV in the valence band originates from the contribution of the Zn 4*s* and O 2*s* states, but it is mainly controlled by O 2*s* state. Hence, the deep-level inner-layer electrons belong to O 2*s* states. The higher energy region of the valence band situated from –6 eV to 0 eV is mainly derived from Zn 3*d* and O 2*p* states due to the strong hybridization that occurred between both states. The top region of the valence band is primarily originated from the O 2*p* state. The bottom part of the conduction band above Fermi level is contributed mainly by Zn 4*s* state. The bandgap values are determined by both Zn 4*s* states and O 2*p* states. All the results of wurtzite ZnO from PDOS and TDOS of standard LDA, GGA-PBE and GGA-PBEsol agreed with other reports using DFT [15,48,51].

The inclusion of Hubbard parameter U_d and U_p in LDA+U, GGA-PBE+U and GGA-PBEsol+U calculations led to a downward shift of the hybridized Zn 3*d* and O 2*p* states and tended to upper shifted the bottom conduction band to the broadening bandgap between the highest valence band and lowest conduction band. The Zn 3*d* and O 2*p* states at the higher energy region of the valence band moved to a relevant position about –6.9 eV compared to standard LDA, GGA-PBE and GGA-PBEsol about –6 eV.

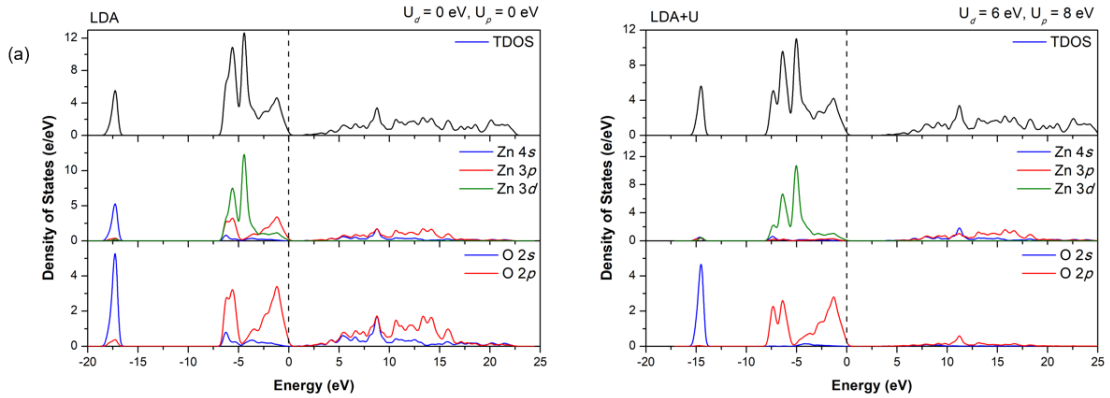

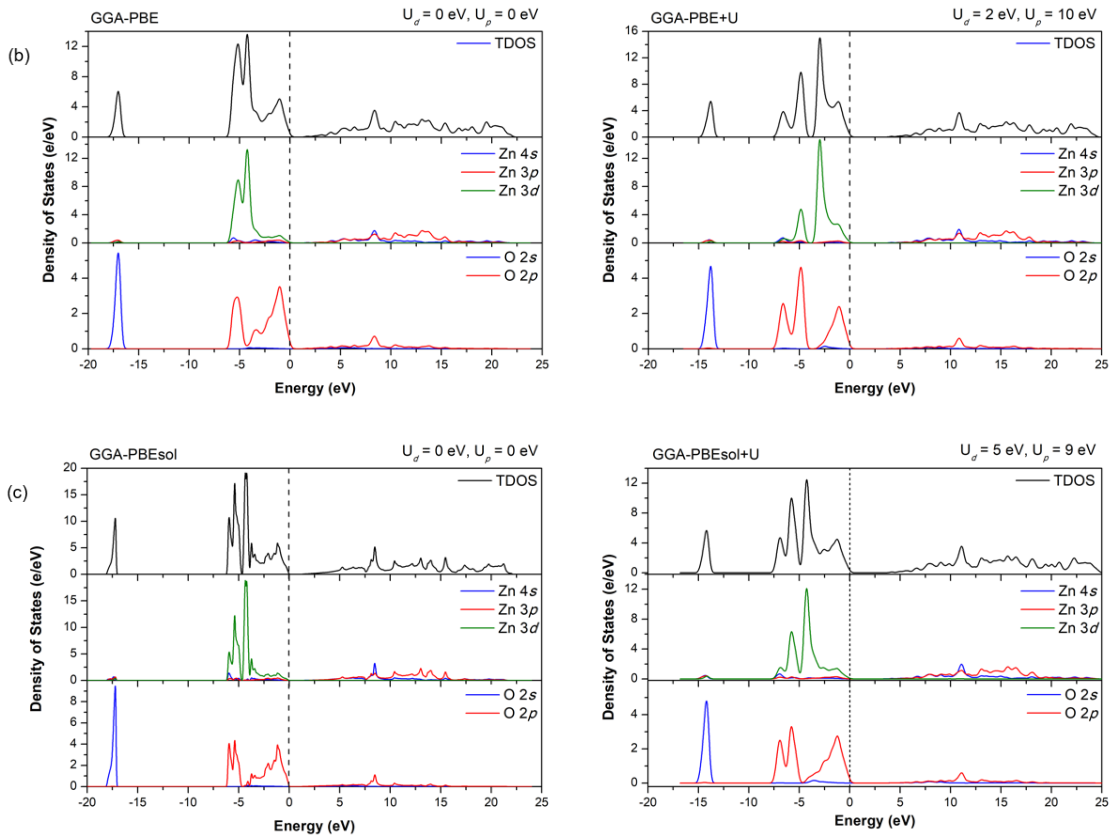

Figure 9: Comparison PDOS and TDOS of wurtzite ZnO using different functionals (a) LDA and LDA+U, (b) GGA-PBE and GGA-PBE+U and (c) GGA-PBEsol and GGA-PBEsol+U for without Hubbard U and with the best Hubbard parameters U_d and U_p

CONCLUSION

In this study, the structural parameters and electronic properties of wurtzite ZnO were evaluated by first-principles calculations based on DFT and DFT+U methods from CASTEP software. The inclusion of Hubbard parameters U_d and U_p in LDA+U, GGA-PBE+U and GGA-PBEsol+U have marked a significant difference in the structural parameters and electronic structure of wurtzite ZnO. The inclusion of Hubbard parameters U_d and U_p have underestimated the lattice parameters and volume of wurtzite ZnO and improved the underestimated bandgap from standard DFT. The calculated lattice parameters and volume were most aptly described from GGA-PBEsol+U functional with possible agreements of different Hubbard U_d and U_p values. The best Hubbard parameters of wurtzite ZnO found for functionals LDA+U at U_d = 6 eV and U_p = 8 eV, GGA-PBE+U at U_d = 2 eV and U_p = 10 eV and GGA-PBEsol+U at U_d = 5 eV and U_p = 9 eV show a good agreement with the experimental bandgap. DOS calculations were used to investigate the composition that determined the wurtzite ZnO band structure. The O 2*p* state primarily dominates the top part of the valence band and the bottom part of the conduction band is contributed mainly by the Zn 4*s* state. Incorporating the Hubbard parameters U_d and U_p into calculations resulted in a downward shift of the hybridized Zn 3*d* and O 2*p* states and a slight upper shift the

bottom conduction band toward the broadening bandgap between the highest valence band and lowest conduction band. Our results suggest that the predicted GGA-PBEsol+U method for investigating the structural and electronic properties of wurtzite ZnO is acceptable for solving the DFT calculations problem at a low computing cost.

ACKNOWLEDGMENT

The authors would like to acknowledge the Ministry of Higher Education (MOHE) Malaysia for funding this research under the KEPU grant 600-RMC/KEPU 5/3 (008/2021) and Universiti Teknologi Mara (UiTM), Cawangan Selangor, Dengkil, Selangor, Malaysia and Faculty of Applied Sciences, Universiti Teknologi MARA, Shah Alam, Selangor, Malaysia for providing the facilities and support on this research.

REFERENCES

[1] R. Vittal and K. C. Ho (2017) *Renew. Sust. Energ. Rev.* **70**, 920.
[2] B. Mehmood, M. I. Khan, M. Iqbal, A. Mahmood and W. Al-Masry (2021) *Int. J. Energ. Res.* **45**(2), 2445.
[3] J. C. Fan, K. M. Sreekanth, Z. Xie, S. L. Chang and K. V. Rao (2013) *Prog. Mater. Sci.* **58**(6), 874.
[4] Y. Segawa, A. Ohtomo, M. Kawasaki, H. Koinuma, Z. K. Tang, P. Yu and G. K. L. Wong (1997) *Phys. Status Solidi* **202**(2), 669.
[5] C. W. Litton, D. C. Reynolds and T. C. Collins (2011) *Zinc Oxide Materials for Electronic and Optoelectronic Device Applications*, United Kingdom, Wiley.
[6] E. Cerrato, C. Gionco, M. C. Paganini and E. Giamello (2017) *J. Phys. Condens. Matter* **29**(44), 444001.
[7] J. B. Baxter, A. M. Walker, K. Van Ommering and E. S. Aydil *Nanotechnology* **17**(11), S304.
[8] Ü. Özgür, Y. I. Alivov, C. L. A. Teke, M. A. Reshchikov, S. Doğan, V. Avrutin, S.-J. Cho and H. Morkoç (2005) *J. Appl. Phys.* **98**, 041301.
[9] K. Bashyal, C. K. Pyles, S. Afroosheh, A. Lamichhane and A. T. Zayak (2018) *J. Phys. Condens. Matter* **30**, 065501.
[10] Z. Alahmed and H. Fu (2008) *Phys. Rev. B* **77**, 045213.
[11] Z. Li, Y. Xu, G. Gao, T. Cui, and Y. Ma (2009) *Phys. Rev. B* **79**, 193201.
[12] J. P. Perdew (1985) *Int. J. Quantum Chem.* **28**(S19), 497.
[13] J. P. Perdew, K. Burke and M. Ernzerhof (1996) *Phys. Rev. Lett.***77**, 3865.
[14] A. Janotti and C. G. Van De Walle (2009) *Reports Prog. Phys.* **72**(12), 125501.
[15] A. A. Mohamad, M. S. Hassan, M. K. Yaakob, M. F. Mohamad Taib, F. W. Badrudin, O. H. Hassan and M. Z. A. Yahya (2017) *J. King Saud Univ. - Eng. Sci.* **29**(3), 278.
[16] S. Lany and A. Zunger (2009) *Model. Simul. Mater. Sci. Eng.* **17**(8), 084002.
[17] B. Yamina, A. Abderrahim, B. Omar and B. Lazhar (2018) *Der. Pharma. Chem.* **10**(1), 16.
[18] V. I. Anisimov, J. Zaanen and O. K. Andersen (1991) *Phys. Rev. B* **44**, 943.
[19] V. I. Anisimov, F. Aryasetiawan and A. I. Lichtenstein (1997) *J. Phys. Condens. Matter* **9**(4), 767.

[20] V. Ivády, K. Szasz, A. L. Falk, P. V. Klimov, D. J. Christle, E. Janzén, I. Abrikosov, D. D. Awschalom and A. Gali (2015) *Phys. Rev. B.* 92(11), 115206.
[21] J. Heyd, G. E. Scuseria and M. Ernzerhof (2003) *J. Chem. Phys.* **118**, 8207.
[22] M. Shishkin, M. Marsman and G. Kresse (2007) *Phys. Rev. Lett.* **99**, 246403.
[23] P. J. Hasnip, K. Refson, M. I. J. Probert, J. R. Yates, S. J. Clark and C. J. Pickard (2014) *Philos. Trans. R. Soc. A* **372**, 20130270.
[24] R. Farooq, T. Mahmood, A. W. Anwar and G. N. Abbasi (2016) *Superlattices Microstruct* **90**, 165.
[25] X. H. Zhou, Q. Hu and Y. Fu (2008) *J. Appl. Phys.* **104**, 063703.
[26] Y. S. Lee, Y. C. Peng, J. H. Lu, Y. R. Zhu and H. C. Wu (2014) *Thin Solid Films* **570**, 464.
[27] R. M. Sheetz (2009) *Phys. Rev. B* **80**, 195314.
[28] E. S. Goh, J. W. Mah and T. L. Yoon (2017) *Comput. Mater. Sci.* **138**, 111.
[29] V. N. Jafarova, G. S. Orudzhev & U. Hubbard (2021) *Solid State Commun.* **325**, 114166.
[30] M. D. Segall, P. J. D. Lindan, M. J. Probert, C. J. Pickard, P. J. Hasnip, S. J. Clark and M. C. Payne (2002) *J. Phys.: Condens. Matter* **14**, 2717.
[31] J. P. Perdew and Y. Wang (1992) *Phys. Rev. B* **45**, 13244.
[32] J. P. Perdew and A. Zunger (1981) *Phys. Rev. B* **23**, 5048.
[33] J. P. Perdew, A. Ruzsinszky, G. I. Csonka, O. A. Vydrov, G. E. Scuseria, L. A. Constantin, X. Zhou and K. Burke (2008) *Phys. Rev. Lett.* **100**, 136406.
[34] G. J. Shao (2009) *J. Phys. Chem. C* **113**(16), 6800.
[35] J. Wang, T. Shen, Y. Feng and H. Liu (2020) *Phys. B: Condens. Matter* **576**, 411720.
[36] J. Q. Wen, J. M. Zhang, Z. G. Qiu, X. Yang and Z. Q. Li (2018) *Phys. B Condens. Matter* **534**, 44.
[37] M. K. Yaakob, N. H. Hussin, M. F. M. Taib, T. I. T. Kudin, O. H. Hassan, A. M. M. Ali and M. Z. A. Yahya (2014) *Integr. Ferroelectr.* **155**, 15.
[38] K. Harun, F. Hussain, A. Purwanto, B. Sahraoui, A. Zawadzka and A. A. Mohamad (2017) *Mater. Res. Express* **4**(12), 122001.
[39] S. Desgreniers (1998) *Phys. Rev. B* **58**, 14102.
[40] K. Harun, M. K. Yaakob, M. F. M. Taib, B. Sahraoui, Z. A. Ahmad and A. A. Mohamad (2017) *Mater. Res. Express* **4**(6), 085908.
[41] X. Ma, Y. Wu, Y. Lv and Y. Zhu (2013) *J. Phys. Chem. C* **117**, 26029.
[42] C. Xia, F. Wang and C. Hu (2014). *J. Alloys Compd.* **589**, 604.
[43] J. Wu, L. Shao, J. Xu and J. Hu (2015) *Sci. Semicond. Process.* **29**, 245.
[44] K. Harun, N. Mansor and M. Kamil (2016) *J. Sol-Gel Sci. Technol.* **80**, 56.
[45] H. C. Wu, H. H. Chen and Y. R. Zhu (2016) *Materials (Basel).* **9**(8), 647.
[46] H. Zhang, S. Lu, W. Xu and F. Yuan (2014) *Surf. Sci.* **625**, 30.
[47] L. Li, W. Wang, H. Liu, X. Liu, Q. Song and S. Ren (2009) *J. Phys. Chem. C* **113**(19), 8460.
[48] C. Zuo, J. Wen and C. Zhong (2012) *J. Semicond.* **33**(7), 072001.
[49] L. Honglin, L. Yingbo, L. Jinzhu and Y. Ke (2014) *J. Alloys Compd.* **617**, 102.
[50] Z. Ma, F. Ren, X. Ming, Y. Long and A. A. Volinsky (2019) *Materials* **12**(1), 196.
[51] F. Xie, P. Yang, P. Li and L. Zhang (2012) *OPTICS* **285**, 2660.